

Design of macro-filter-lens with simultaneous chromatic and geometric aberration correction

Dilip K. Prasad^{1,*} and Michael S. Brown¹

¹*School of Computing, National University of Singapore, Singapore 117417*

compiled: November 25, 2013

A macro-filter-lens design that can correct for the chromatic aberration and geometric aberration simultaneously while providing long focal length is presented. The filter is easy to fabricate since it involves two spherical surfaces and a planar surface. Chromatic aberration correction is achieved by making all the rays travel the same optical distance inside the filter element (negative meniscus). Geometric aberration is corrected by the lens element (plano-convex) which makes the output rays parallel to the optic axis. This macro-lens filter design does not need additional macro lens and provides an inexpensive and optically good (aberration compensated) solution for macro imaging of objects not placed close to the camera.

OCIS codes: (090.1000) Aberration compensation; (220.3620) Lens system design; (350.2450) Filters, absorption.

<http://dx.doi.org/10.1364/XX.99.099999>

1. Introduction

Macrophotography is an interesting photography mode in which the object is of the same length scale as the camera sensor and is typically very close to the camera. While there are dedicated single focal length or variable focal length macro lens systems, they are generally very expensive (often heavy too) and thus bought mostly by professional photographers. However, for amateur photographers and photography enthusiasts, the expectation from the digital cameras is ever-increasing and they often desire good quality and diverse photography capability at an investment of small additive cost. In terms of macrophotography, it often translates to being able to perform macrophotography by combining cheap lenses and filters with camera's default lenses, being able to take macro from long distances (typically more than 10 - 15 cm), having little chromatic and geometric aberrations, etc, even while not needing several separate optical components.

Expectedly, the cheaper optics (lenses and filters) perform poorer than the optics dedicated to macrophotography. The reason is that the dedicated macrophotography optics satisfy stringent optical goals by employing complex designs and several

lenses/filters [1, 2]. And thus expectedly, the cost and weight of such dedicated optics is high. On the other hand, simple and inexpensive design may suffer from some undesirable characteristics, such as chromatic aberration, spherical aberration, distortion, etc. For example, having invested in a macro lens, if a photographer combines it with a general color filter (which is a planar slab), the chromatic aberration introduced due to the filter is significant for macrophotography [3], though it may not have mattered a lot in the general photography. However, such problems can be circumvented by simple and elegant solutions, such as provided by [3] for the above mentioned problem of chromatic aberration of a filter in macrophotography. Thus, we refer to [3]'s filter design as macro-filter.

Our work is inspired by [3]. Ref. [3]'s macro-filter for macrophotography has a design such that each ray travels approximately the same path length inside the filter, such that the filter does not introduce significant chromatic aberration. By design, this macro-filter is good for the cases where the object is very close ($W < R$ in Fig. 1) to the lens. For example, for a filter with $R = 100\text{mm}$, the practical working distance would range from 10–100mm. Lastly, for using this filter, an additional close up (macro) lens is needed along with the camera lens system.

* Corresponding author: dilipprasad@gmail.com

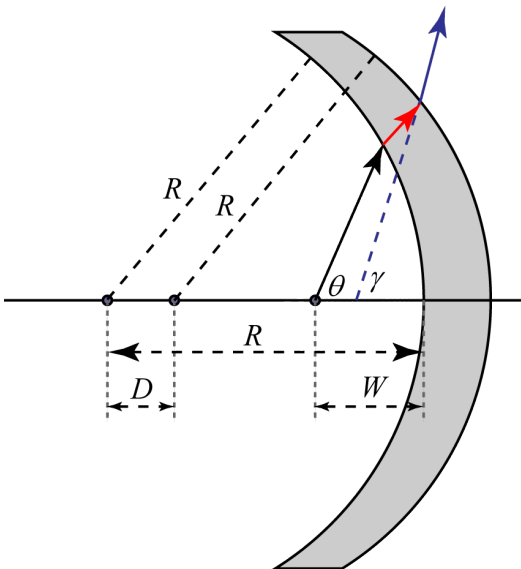


Fig. 1. Illustration of the macro-filter design proposed in [3]. Here, approximate path travelled by the rays $D \ll R$, working distance $W < R$, R is the radius of the two spherical surfaces, and n is the filter material.

In this paper, we work further on the problem of simple optics for macrophotography. Here we consider the problem of macrophotography when the object of interest cannot be brought very close to the camera. We propose a simple design consisting of two optical elements sharing a common surface such that the filter itself can function as a macro lens. Thus, we call the proposed element as macro-filter-lens.

The outline of the paper is as follows. Section 2 presents the proposed design. Section 3 verifies the design goals. Section 4 presents simulations of practical quantities using ray tracing software Zemax and section 5 concludes the paper.

2. Proposed macro-filter-lens

2.A. Introduction to the proposed design and design goals

The design in [3] is based on the Beer-Lambert law which relates the relative transmission strength for a ray with wavelength λ to the absorption coefficient of the filter's material [4–7]. The goal is achieved using a positive meniscus filter composed of two spherical surfaces of same radius R and having a small distance D between their centers placed along the optic axis, see Fig. 1. For later convenience, we define $a = (R - W)/R$ as the working distance ratio of [3]'s macro-filter. Since the outgoing ray from the filter are diverging, an additional close up (macro) lens is needed to collect the rays

and direct them to the camera's lens system for forming an image on the camera's sensor. Then, the focal point of the macro lens determines the actual working distance of the filter.

Fig. 2 shows the basic design of the proposed filter. The first optical element, if having chromatic properties, works as a filter, though it may be a simple wideband material as well. The first element is the same as the macro-filter of [3], however placed such that the convex surface of this macro-filter faces the object. The second optical element's is a plano convex lens, whose function is to collect the light from the first element and give a collimated output corresponding to the rays coming from the object at the desired focal point, such that an additional macro lens is not necessary.

The two spherical surfaces are of radius R . The first element has refractive index n_1 and may have frequency dependent path losses. The second element, the plano convex lens, is made of clear glass with uniform losses across the visible frequency band. It has refractive index $n_2 > n_1$ and shares the back spherical surface of the filter. The working distance is W and the spherical surface offset is $D \ll R$, which is also the approximate path length travelled by any ray inside the filter material.

The proposed macro-filter-lens design should meet the following goals:

1. The object is quite far from the macro-lens-filter,
2. The output of the macro-lens-filter is approximately collimated so that it can be used with the existing camera lens directly,
3. The chromatic aberration is comparable or lesser than the macro-filter of [3] having same R , D , and $n = n_1$, and
4. The spherical aberration is comparable or lesser than the macro-filter of [3] having same R , D , and $n = n_1$.

2.B. Details of geometry of the macro-filter-lens

A detailed illustration of the proposed macro-filter-lens is shown in Fig. 3. Origin O is the focal point of the macro-filter-lens. O_A and O_B are the centers of the first (C1) and second (C2) curved surfaces, respectively. Both curved surfaces are spherical with radius R . The distance between O_A and O_B is D . The working distance, i.e. distance of O from the

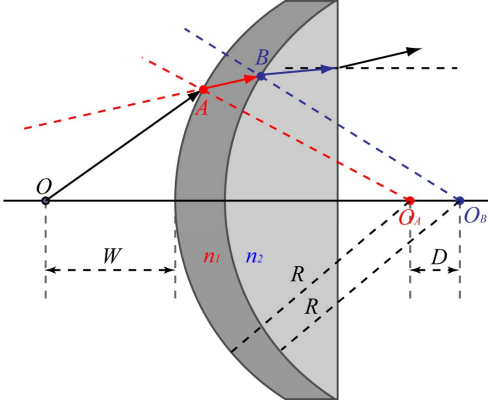


Fig. 2. A basic illustration of the proposed macro-lens-filter.

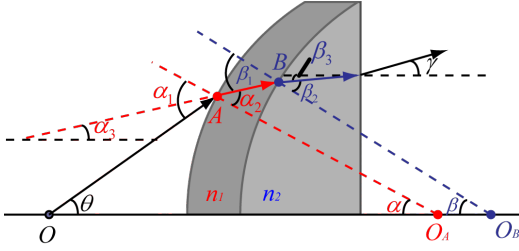


Fig. 3. Detailed illustration of the proposed macro-lens-filter. The definition of all the angles involved in analysis of the macro-lens-filter design are shown here.

C1, is W . Using rigorous ray analysis, we determine the values of various angles can be determined in terms of θ , a , and d as follows. For simplicity of expression, we assign:

$$a = (R + W)/R, \quad d = D/R. \quad (1)$$

We refer to a as the working distance ratio. The first curved surface, C1, can be represented as follows:

$$\begin{aligned} x &= R(a - \cos \alpha), \\ y &= R \sin \alpha. \end{aligned} \quad (2)$$

The second curved surface, C2, can be represented as follows:

$$\begin{aligned} x &= R(a + d - \cos \beta), \\ y &= R \sin \beta. \end{aligned} \quad (3)$$

The ray emanating from the origin O along the angle θ is expressed as

$$y = x \tan(\theta). \quad (4)$$

2.C. Ray analysis

The ray reaches the first curved surface $C1$ and experiences refraction at the point A . The ray trans-

mitted after refraction inside material n_1 reaches the second curved surface $C2$ at B . It experiences another refraction here and the transmitted ray then travels in material n_2 and reaches the planar surface P . Here, it is refracted one more time and comes out of the macro-filter-lens.

The angles $\alpha, \alpha_1, \alpha_2, \alpha_3$ corresponding to surface C1 satisfy the following relationships:

$$\alpha_1 = \alpha + \theta, \quad \alpha_3 = \alpha_2 - \alpha, \quad (5)$$

$$\sin \alpha_1 = n_1 \sin \alpha_2. \quad (6)$$

Here, eq. (5) are from geometry while eq. (6) is due to the Snell's law. Similarly, the angles $\beta, \beta_1, \beta_2, \beta_3$ corresponding to surface C1 satisfy the following relationships:

$$\beta_1 = \alpha_3 + \beta, \quad \beta_3 = \beta_2 - \beta, \quad (7)$$

$$\sin \beta_1 = \frac{n_2}{n_1} \sin \beta_2. \quad (8)$$

Finally, Snell's law at the planar surface gives:

$$\sin \gamma = n_2 \sin \beta_3 \quad (9)$$

For convenience, we define a hypothetical real-valued angle ψ such that

$$a \sin \theta = \sin \psi. \quad (10)$$

Thus, for real-valued angle ψ , $\theta_{\max} = \max(\theta) = \arcsin\left(\frac{1}{a}\right)$.

Using eqs. (2) and (10), we get $\alpha = \psi - \theta$. Then using eq. (5), $\alpha_1 = \psi$. Other angles for C1 can be computed using eqs. (5) and (6). Then for C2, using eqs. (3) and (5), we get:

$$\beta = \arcsin(\sin \alpha_2 + d \sin \alpha_3) - \alpha_3. \quad (11)$$

Further, using eq. (7), we get:

$$\beta_1 = \arcsin(\sin \alpha_2 + d \sin \alpha_3). \quad (12)$$

Then, β_2, β_3 , and γ can be computed using eqs. (8), (7), and (9), respectively.

It is notable that at each point of refraction, only the transmitted ray is being considered and the reflected ray is being neglected. For the curved surfaces C1 and C2, the reflected ray diverges away and does not contribute to the resultant image. For the reflection at the planar interface, the reflected beam refracts again at the surface C2 and eventually diverges away without contributing to the image.

Lastly, the numerical aperture of the macro-lens-filter is small (plotted in Fig. 4). Thus, paraxial approximation applies and the Fresnel transmission coefficients for s and p polarized rays are approximately the same. In other words, polarization induced effects are also insignificant.

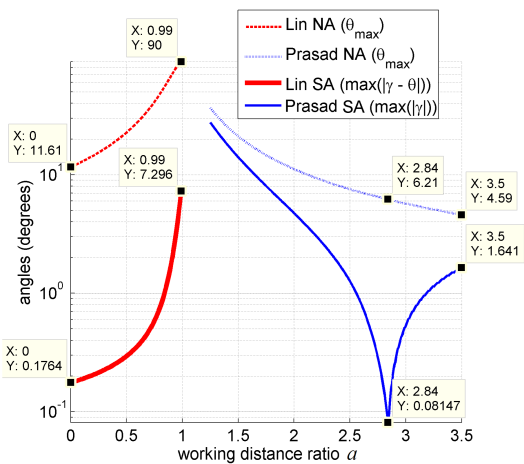


Fig. 4. The numerical aperture (NA) and spherical aberration (SA) of [3]’s macro-filter and the proposed (Prasad) macro-lens-filter design as a function of the working distance ratio.

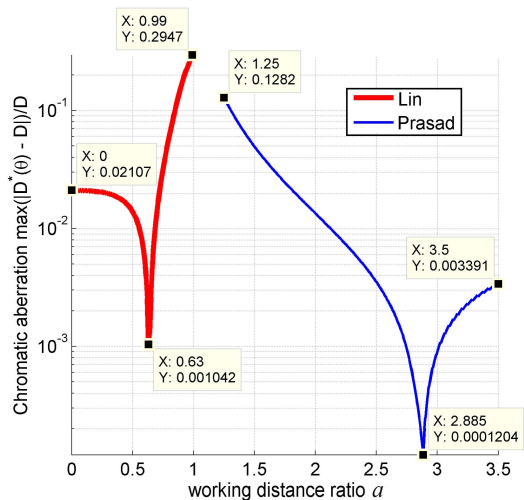


Fig. 5. The chromatic aberration of [3]’s macro-filter and the proposed (Prasad) macro-lens-filter design as a function of the working distance ratio.

3. Verification of the design goals

For verifying the goals, we consider longpass filter material OG530 [8] ($n, n_1 = 1.51$) from Schott AG, Germany as the filter material, and ultra white glass B270 [9] ($n_2 = 1.5229$), also from Schott AG, Germany. We consider $R = 100\text{mm}$, $D = 3\text{mm}$ (i.e. $d = 0.03$) and the filter aperture to be 40mm diameter. These values are used for both [3]’s macro-filter and proposed macro-lens-filter.

Since one of the aims is to make the rays nearly collimated at the output of the macro-lens-filter, it is desirable for that γ is as close to 0 as possible. Thus, $|\gamma|$ can be used as the measurement of spher-

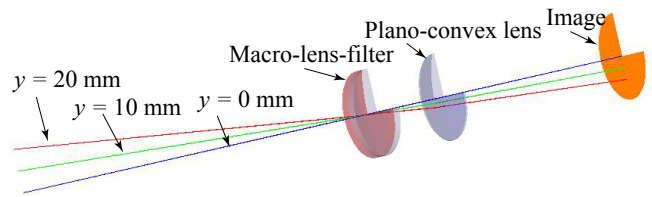


Fig. 6. Illustration of the simulation setup used for Zemax simulation. The front element is the macro-lens-filter, the back element is the plano-convex lens used for focusing the rays from the macro-lens-filter. Red, green, and blue lines indicate rays from three field points corresponding to $y = 0\text{mm}$, $y = 10\text{mm}$, $y = 20\text{mm}$.

ical aberration (SA) for this macro-lens-filter. On the other hand, the SA of [3]’s macro-filter can be measured as $|\gamma - \theta|$. Further, the chromatic aberration can be quantified as $\frac{|D^*(\theta) - D|}{D}$, where $D^*(\theta)$ is the path length AB of the ray inside the filter material. The maximum chromatic aberration $\frac{\max(|D^*(\theta) - D|)}{D}$ is studied.

The numerical aperture (NA) and the spherical aberration of the proposed macro-lens-filter and [3]’s macro-filter are plotted in Fig. 4. The chromatic aberration of the proposed macro-lens-filter and [3]’s macro-filter are plotted in Fig. 5.

It is seen that [3]’s macro-filter provides larger NA than our macro-lens-filter. This is quite expected since [3]’s macro-filter is placed very close to the object while our macro-lens-filter is placed at a significant distance from the object. It is notable that the available numerical aperture can be increased for both the proposed macro-lens-filter and [3]’s macro-filter by using the working distance ratio a close to 1. However, the chromatic and spherical aberrations are very high for values of a closer to 1. So, such working distances are not preferred.

The proposed macro-lens-filter can achieve lesser geometric and chromatic aberrations than [3]’s filter for a certain range of values of a , i.e. $a \in [2.795, 2.875]$. In general, the aberrations are quite low in the range $a \in [2.7, 3.0]$, which translate to working distance range of $W \in [170, 200]\text{mm}$. This indicates large focal length for macro photography and large depth of focus as well. Indeed the working distance range can be scaled to larger values by using a larger value of R , however at the cost of the numerical aperture.

4. Simulation using ray-tracing software

We simulated some important parameters using the ray tracing software Zemax. Since the proposed macro-lens-filter results in rays parallel to the op-

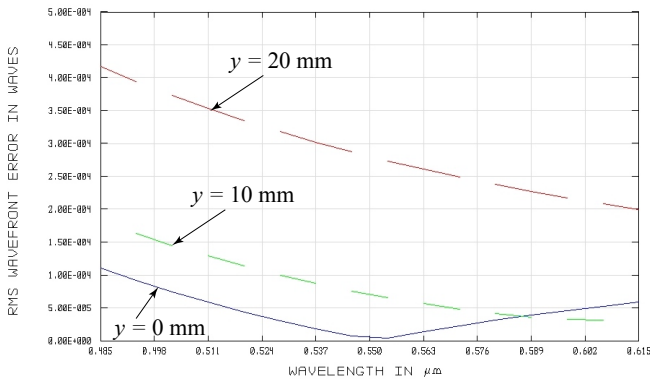


Fig. 7. RMS errors are plotted as a function of wavelength. Blue, green, and red lines indicate rays from three field points corresponding to $y = 0\text{mm}$, $y = 10\text{mm}$, $y = 20\text{mm}$.

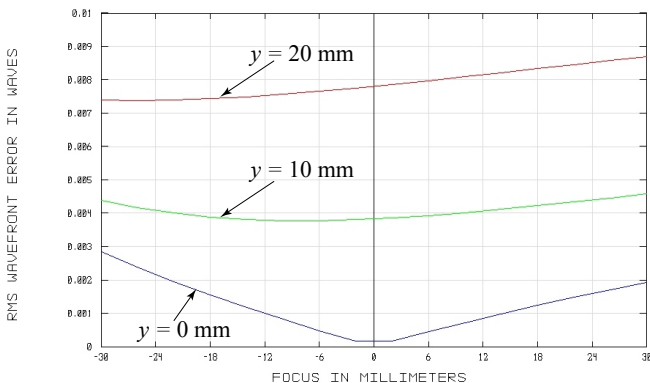


Fig. 8. RMS errors are plotted as a function of longitudinal deviation from the focal point. Blue, green, and red lines indicate rays from three field points corresponding to $y = 0\text{mm}$, $y = 10\text{mm}$, $y = 20\text{mm}$.

tic axis, we place a simple plano-convex lens after the macro-lens-filter while simulation so that a practical image plane can be formed and used for simulating useful parameters. A better and sophisticated lens for collecting the rays will have lower aberrations, but we use a simple lens to show that the aberrations are indeed quite small even when a simple lens is used for collection. The plano-convex lens has a focal length of 95 mm and the curved surface faces the planar surface of the macro-lens-filter. An illustration is shown in Fig. 6.

Figure 7 shows the root mean square (RMS) error plotted as a function of the wavelength. It is notable that the smaller wavelengths have higher error. As expected, field point further away from the optic axis have higher errors. Nevertheless, the maximum error is 4.15×10^{-4} .

Figure 8 shows the root mean square (RMS) error

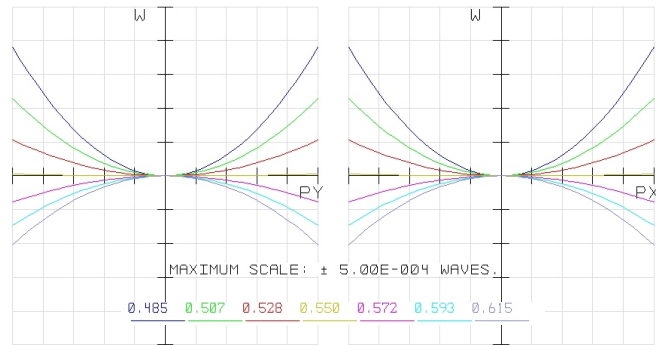


Fig. 9. Optical path differences are plotted as a function of pupil angle and for various wavelength (unit μm) samples in the visible range.

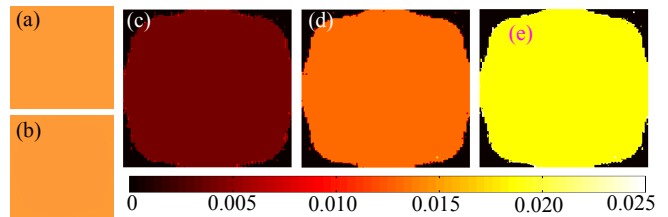


Fig. 10. Difference between the color channels of the object and image planes. (a) object plane, (b) image plane, (c) difference in red channel, (d) difference in green channel, (e) difference in blue channel.

plotted as a function of the longitudinal deviation from the focal point. It is seen that the RMS error is quite small for a long range of deviation from the focal point (60 mm) and the largest error is 0.0087. This indicates that the approach works well and has consistent long range characteristics.

Figure 9 shows the optical path difference (OPD) plotted as a function of the pupil angle. It is seen that the OPDs are the largest for smaller wavelengths. The OPDs are significantly small, largest being close to 0.0004 waves which indicates hardly any spherical aberration. Further, though the variation in the OPDs is relatively large over different wavelengths, due to very small values, it is expected to be quite small.

In order to verify this, we consider an orange colored surface ($R = 255$, $G = 155$, $B = 55$, R,G,B: red, green, blue color channels respectively) placed at the object plane and compare it with the image obtained. Figure 10(a,b) show the object and image planes. For quantitative comparison, we show the relative difference (for example $|1 - R(\text{image})/R(\text{object})|$) between the color values of the red and green channels in Fig. 10(c,d). Since OG530 is a low pass filter, the blue channel should

be attenuated significantly. However, for the sake of comparison of chromatic aberration, considering no attenuation, we compare the blue channel as well in Fig. 10(e). The maximum relative difference appears for the blue channel that corresponds to smaller wavelengths. This can be verified in Fig. 7 as well, where it is seen that smaller wavelengths have larger RMS errors. The maximum errors for red and green channels are 1.2% and 1.8% respectively, which are significantly smaller than the approximate maximum errors for [3]’s design, which are 14.8% and 17.0% respectively.

5. Conclusion

In conclusion, the proposed macro-lens-filter deals with chromatic aberration and spherical aberration quite well, while providing large working distance and depth of focus. The design is verified using ray tracing software Zemax and it is shown that the aberrations are indeed quite small for the design. Such a simple design is easy to fabricate and thus expected to have significant advantage over dedicated macro-optics. Further, by integration of filter and lens function in a single optic, it is handier to use. We believe on the principle that a reasonable optical performance can be achieved using simple and elegant designs such that the power of optics can be made available to non-expert users at low cost. This macro-lens-filter design exemplifies this belief.

Acknowledgement

This study was funded by Agency for Science, Technology and Research (grant no. 1121202020). The

authors thank Dr. Zhang from Nanyang Technological University for the help in Zemax software.

References

- [1] D. Miller, How complicated must an optical component be?, *Journal of the Optical Society of America A* **30**, 238 (2013).
- [2] S. Pal, Aberration correction of zoom lenses using evolutionary programming, *Applied Optics* **52**, 5724 (2013).
- [3] Y.-H. Lin, J.-Y. Lai, H.-Y. Tsai, H.-C. Chang, H. Huang, Y.-F. Chen, and K.-C. Huang, Optical imaging with spectrum aberration correction using a filtering macrolens, *Applied Optics* **52**, 5058 (2013).
- [4] D. Skoog, F. Holler, and S. Crouch, *Principles of Instrumental Analysis* (Brooks/Cole, 2007).
- [5] R. Tagirov and L. Tagirov, Lambert formula - Bouguer absorption law?, *Russian Physics Journal* **40**, 664 (1997).
- [6] A. Ryer, *Light Measurement Handbook* (International Light, 1997).
- [7] S. Dew and R. Parsons, Absorbing filter to flatten Gaussian beams, *Appl. Opt.* **31**, 3416 (1992).
- [8] Schott, “Longpass filters,” http://www.schott.com/advanced_optics/english/products/filteroverviewdetaillongpass.html ().
- [9] Schott, “B 270 i ultra-white glass,” http://www.schott.com/advanced_optics/english/syn/advanced_optics/products/optical-materials/thin-glass/flat-glass-b-270/index.html ().